Synthesis and Structural Investigation of Zr(BH4)(4)

L.H. Rude; M. Corno; P. Ugliengo; M. Baricco; Y.S. Lee; Y.W. Cho; F. Besenbacher; J. Overgaard; T.R. Jensen. Synthesis and Structural Investigation of Zr(BH4)(4). JOURNAL OF PHYSICAL CHEMISTRY. C, NANOMATERIALS AND INTERFACES. 116 pp: 20239-20245.
DOI: 10.1021/jp306665a

Synthesis and structural investigation of $Zr(BH_4)_4$

Line H. Rude,[1] Marta Corno,[2] Piero Ugliengo,[2] Marcello Baricco,[2] Young-Su Lee,[3] Young Whan Cho,[3] Jacob Overgaard,[1] and Torben R. Jensen[1,*]

[1] *Center for Materials Crystallography, Interdisciplinary Nanoscience Center and Department of Chemistry, Aarhus University, Langelandsgade 140, DK-8000 Århus C, Denmark*
[2] *Dipartimento di Chimica and NIS, Università di Torino, Torino, Italy*
[3] *High Temperature Energy Materials Research Center, Korea Institute of Science and Technology, Seoul 136-791, Republic of Korea.*

* Corresponding author: trj@chem.au.dk , Tel: +45 8942 3894, Fax: +45 8619 6199

Abstract

Zirconium tetraborohydride, $Zr(BH_4)_4$ was synthesized by a metathesis reaction between $LiBH_4$ and $ZrCl_4$ using high energy ball milling. Initially, a white powder was produced and during storage at -30 °C in a closed vial transparent rectangular single crystals formed under the lid by vapor deposition. Single crystal X-ray diffraction data revealed a cubic unit cell (a = 5.8387(4) Å, space group P-43m, determined at T = 100 K), which consist of neutral $Zr(BH_4)_4$ molecules. The BH_4^- anions coordinate to Zr via the tetrahedral faces (η_3). The shortest distance between neighboring molecules in the solid is defined by B–H2···H2–B interactions of 2.77 Å. DFT calculations, based on the experimental structure, have been performed with the CRYSTAL code. A phonon instability in the Γ point was observed for space group symmetry P-43m, which can eliminated by a symmetry reduction to the cubic space group P23, suggesting an orientational disorder of BH_4^- tetrahedral in the structure. Computed IR spectra for the two structural models turned out to be very similar. Synthesis and decomposition was further investigated using *in situ* synchrotron radiation powder X-ray diffraction.

Keywords: Zirconium tetraborohydride, Structural investigation, Single crystal X-ray diffraction, In situ synchrotron powder X-ray diffraction, Computer simulation.

1. Introduction

Metal borohydride materials are receiving increasing interest as potential hydrogen storage materials due to their high volumetric and gravimetric hydrogen densities. Recently, a number of novel double cation or double anion metal borohydrides was discovered with a variety of new structures.[1–8] Monometallic borohydrides usually form framework structures, however, they may also form molecular structures when the metal has an oxidation state ≥ 3, e.g. $Al(BH_4)_3$ and $Zr(BH_4)_4$. The molecular metal borohydrides have low melting and boiling points and tend to decompose at temperatures slightly above room temperature. Zirconium tetraborohydride melts at 29 °C and the hydrogen release temperature is reported to be 167 °C.[9,10] Despite the heavy metal, Zr, center in the molecule zirconium borohydride, $Zr(BH_4)_4$, still has a very high hydrogen content of ρ_m = 10.7 wt% H_2 and ρ_V = 108 kg H_2/m^3. Several synthesis approaches has been reported, e.g. by a reaction between $Al(BH_4)_3$ and $ZrCl_4$. Aluminium borohydride also reacts with the double salt $NaZrF_5$ in ether solution to form $Zr(BH_4)_4$, NaF and AlF_2BH_4.[9] Furthermore, a metathesis reaction between $LiBH_4$ and $ZrCl_4$ is a straight forward procedure for preparation of $Zr(BH_4)_4$, according to reaction scheme (1):[11,12]

$$ZrCl_4(s) + 4LiBH_4(s) \rightarrow Zr(BH_4)_4(s) + 4LiCl(s) \quad (1)$$

Reaction (1) may be mechano-chemically facilitated, i.e. by high energy ball milling, which has been proven to be an important method for preparation and modification of novel hydrogen rich compounds.[13,14] Different mechano-chemical methods have recently been used to synthesize $Zr(BH_4)_4$ via reaction (1). Detailed structural characterization of $Zr(BH_4)_4$ has been hampered by the limited quality of the product and the volatile nature of molecular borohydrides.[10,12] Today, there is limited knowledge on the molecular borohydrides, which has prompted the present investigation. In this paper a new synthesis route for molecular borohydrides is presented along with detailed structural investigations of $Zr(BH_4)_4$ combining single crystal X-ray diffraction and

DFT optimization of the geometry. The vibrational spectra of $Zr(BH_4)_4$ are calculated and measured and the decomposition mechanism is investigated using in situ synchrotron radiation powder X-ray diffraction.

2. Experimental

Two samples were prepared, $LiBH_4$–$ZrCl_4$ (4:1, S1) and (6:1, S2) containing 20 and 14 mol% $ZrCl_4$, respectively, using the chemicals $LiBH_4$ (95%, Aldrich) and $ZrCl_4$ (99.5%, Alfa Aesar). The samples were mixed by high energy ball milling (BM) for in total 6 min at 300 rpm (1 min BM followed by 2 min break, 6 repetitions) using a Fritsch pulverisette no. 4. Tungsten carbide (WC) vial (80 mL) and balls (10 mm) were used and the sample-to-ball mass ratio was 1 : 30. The vial, loaded with balls and powder was cooled to −30 °C prior to ball milling to prevent over-heating of the sample. The samples were stored at −30 °C and transparent single crystals with rectangular shape (up to ~2 mm) formed under the lid by vapor deposition after ca. 14 to 30 days.

A single crystal (approximate dimensions 0.25, 0.13 and 0.08 mm) was collected from the lid of the vial containing sample S1 and mounted inside a 0.5 mm glass capillary. The capillary was sealed by a composite adhesive to prevent contact with air and rapidly transferred to the cryostream (T = 100 K) on a Bruker X8 APEX2 diffractometer. The diffraction data were collected on an APEX2 CCD detector using a fine-focus sealed tube diffraction source with MoKα radiation (λ = 0.71073 Å). All data reduction was performed with the Bruker APEX2 suite of programs. Heavy atoms were located by direct methods using SHELXS while hydrogen atoms were found from difference Fourier synthesis and subsequently the positions and isotropic parameters for the two hydrogen atoms were refined independently using SHELXL.[15] Several measurements were performed before satisfactory data was collected due to the volatile nature of $Zr(BH_4)_4$ at *RT* and its sensitivity towards air.

In situ time-resolved synchrotron radiation powder X-ray diffraction (SR-PXD) data were measured for S2 at the MAX-II synchrotron beamline I711 at MAX-lab, Lund, Sweden with a MAR165 CCD detector system (λ = 0.9450 Å).[16] The sample was mounted in a sapphire (Al_2O_3) single crystal tube (1.09 mm o.d., 0.79 mm i.d.).[17] The X-ray exposure time was 30 s per PXD pattern and the sample was heated from 19 to 60 °C (heating rate 2.5 °C/min) in argon atmosphere. The data were integrated using the Fit2D program [18] and analyzed by Rietveld refinement with the Fullprof suite.[19]

FTIR spectra were collected for $LiBH_4$–$ZrCl_4$ (4:1, S1) using a Bruker ALPHA FT-IR spectrometer. The measurements were performed in an argon-filled glove box at *RT* in the time period 0 to 120 min after synthesis of the sample. The spectra were obtained in a 4000–350 cm^{-1} range at 2 cm^{-1} resolution. 24 scans were collected and averaged for each spectrum and for the background.

All handling and manipulation of the chemicals and sample preparations were performed in an argon-filled glove box with circulation purifier, $p(O_2, H_2O)$ < 0.5 ppm and all equipment was cooled to −30 °C prior to handling of the samples.

3. Computational details

Periodic *ab initio* geometry optimization was performed starting with the $Zr(BH_4)_4$ experimental structure as the initial guess. The CRYSTAL09 code [20] was used throughout by adopting the DFT framework. The pure GGA functional PBE [21] and a localized basis set of Gaussian function of polarized triple-zeta quality were used. For zirconium an all-electron 97636-121* basis set was used,[22] while boron and hydrogen were described by the Ahlrichs basis sets.[23] Phonons at Gamma point in the harmonic approximation were computed by the diagonalization of the associated mass-weighted Hessian matrix (for details on the computational procedure see references [24,25]).

Calculations on $Hf(BH_4)_4$ have been performed for comparison. Basis set and functional dependency have been assessed in order to improve the reliability of the results. Details are reported in the Electronic Supplementary Information.

4. Results and discussion

4.1 *Single crystal X-ray diffraction*

The structure of $Zr(BH_4)_4$ was solved from single crystal X-ray diffraction in a cubic crystal system using space group *P*-43*m* and unit cell parameter a = 5.8387(4) Å (T = 100 K). $Zr(BH_4)_4$ is isomorphous to $Hf(BH_4)_4$ [26] and the structure of $Zr(BH_4)_4$ is therefore compared to that of $Hf(BH_4)_4$ in the following. Experimental data, refinement details and crystal data are provided in Table 1 and compared to those obtained in a previous study for $Hf(BH_4)_4$.[26]

Table 1 Crystal data and refinement results for $Zr(BH_4)_4$ compared with the crystal structure of $Hf(BH_4)_4$.

Compound	**$Zr(BH_4)_4$** [a]	**$Hf(BH_4)_4$** [26]
Formula weight /g·mol^{-1}	150.60	237.86
T /K	100	110
Crystal system	Cubic	Cubic
Space group	*P*-43*m*	*P*-43*m*
a /Å	5.8387(4)	5.827(4)
V /Å^3	199.04(4)	197.8
Z, D_c /g·cm^{-3}	1, 1.256	1, 1.997
λ /Å, μ /mm^{-1}	X-ray 0.71073, 1.259	Neutron 1.142(1), 1.299
$2\theta_{max}$ /°, completeness /%	85.76, 97.4	120, -
R_{int}	0.0512	
Reflns collected, unique	2851, 307	162, 99
Restraints, parameters	0, 10	
$R(F^2)_{all}$, $R_w(F^2)_{all}$	0.0154, 0.0296	0.126, 0.185
GOF	1.176	
Largest Fourier diff /e·Å^{-3}	−0.218/0.443	

[a] This work

The unit cell parameter and space group found for $Zr(BH_4)_4$ are in agreement with previous studies.[27] The atomic coordinates determined from single crystal X-ray diffraction are reported in Table 2. The atoms are occupying the same Wyckoff sites as found for $Hf(BH_4)_4$.[26]

Table 2 Atomic coordinates for $Zr(BH_4)_4$ derived from single crystal X-ray diffraction data measured at T = 100 K.

Name	Element	Wyck.	x/a	y/b	z/c
Zr	Zr	1a	1	1	1
B	B	4e	0.7714(2)	0.7714(2)	0.7714(2)
H2	H	4e	0.668(3)	0.668(3)	0.668(3)
H1	H	12i	0.956(4)	0.748(2)	0.748(2)

Zr-ions are positioned at the corners of the cubic unit cell, with four BH_4^- anions in an ideal tetrahedral coordination to Zr (CN = 4), see Figure 1A. The BH_4^- anions are connected to Zr via the tetrahedral faces (η^3), see Figure 1B, as found for the high temperature phase of $LiBH_4$.[28,29] Each BH_4^- anion is coordinated to a single Zr atom (CN = 1).

Selected interatomic distances and angles for $Zr(BH_4)_4$ and $Hf(BH_4)_4$ are compared in Table 3. The boron-boron distances are 3.7752(17) Å for borohydride units coordinated to the same zirconium and the Zr-Zr distances for neighboring molecules are 5.8387(4) Å for $Zr(BH_4)_4$. In both cases, these values are slightly larger than those observed for $Hf(BH_4)_4$. However, the Zr-H and B-H distances in $Zr(BH_4)_4$ are slightly shorter than those found in $Hf(BH_4)_4$. The distances and angles for the BH_4^- complex anions reveal a slightly larger distortion away from the perfect tetrahedral shape for $Zr(BH_4)_4$ than for $Hf(BH_4)_4$. The experimental structural data clearly support previous assumptions that solid $Zr(BH_4)_4$ consists of discrete neutral molecules of $Zr(BH_4)_4$ interacting mainly by weak van der Waals and dispersion interactions. The shortest distance between neighboring molecules in the solid is defined by the H2…H2 distances of 2.77 Å. Four H2 atoms

point towards the center of the unit cell being responsible for the intermolecular interactions in the crystal structure.

The BH_4^- tetrahedron is slightly distorted so that the three H1 hydrogen atoms are displaced towards the Zr atom with an H2-B-H1 angle of 115.1°. Distortion could imply a shorter distance for B-H1 bond with respect to B-H2 bond. This would suggest that the negative charge of the BH_4^- anion has been redistributed so that the three H1 atoms share the extra negative charge and thus that the H1 atoms possess slightly higher negative charges than H2 creating a stronger interaction with the Zr-cation. This furthermore suggests that the H2 atom is close to being neutral, which also reduces the repulsive interactions with the neighboring H2 atoms surrounding the cavity in the unit cell center.

Table 3 Selected interatomic distances and angles determined experimentally from single crystal X-ray diffraction data of $Zr(BH_4)_4$ and compared with $Hf(BH_4)_4$ (M = Zr or Hf).

Compound	**$Zr(BH_4)_4$** [a]	**$Hf(BH_4)_4$** [26]
M-M /Å	5.8387(4)	5.827(4)
M-B /Å	2.3118(12)	2.281(8)
M-H2 /Å	3.358(18)	3.432(17)
M-H1 /Å	2.097(18)	2.130(9)
B-B /Å	3.7752(17)	3.725(12)
B-H2 /Å	1.046(18)	1.150(9)
B-H1 /Å	1.095(12)	1.235(10)
H2-H2 /Å	2.77(2)	2.64(3)
H1-H1 /Å	1.718(17)	1.970(16)
H1-H2 /Å	1.81(3)	1.988(10)
M-B-H1 /°	64.9(7)	67.1(5)
M-H1-B /°	86.9(8)	80.6(6)
B-M-H1 /°	28.2(3)	32.3(3)
H1-B-H1 /°	103.3(12)	105.8(6)
H1-B-H2 /°	115.1(12)	112.9(10)

[a] This work

4.2 *Ab initio calculations*

DFT geometry optimization was performed starting from the experimental structural model of $Zr(BH_4)_4$ presented in Table 1 (space group *P*-43*m*) and the results are reported in Table 4. A comparison with experimental data reported in Tables 2 and 3 shows that there is good agreement with the lattice constant, cell volume and density, which show a discrepancy of about 2 %. For some structural data involving hydrogen atoms, the difference between calculated and experimental values are larger (max 15 %), likely due to the difficulty of fixing the position of H atoms by both experimental and theoretical techniques. It is well-known that covalent interactions between H atoms and its neighbor will displace the density towards the bonded atom and thus bias the bond distance towards shorter values. This is probably less pronounced in the B-H bond compared to, say O-H bonds, as the former can be considered a non-polar bond.

The corresponding set of harmonic frequencies revealed one of them to be imaginary at –254 cm^{-1}, as computed with PBE and triple-zeta basis set, representing a phonon instability at Gamma point. So, it appears that the *P*-43*m* structure represents a saddle point on the potential energy surface. An inspection of the eigenmode associated to the imaginary frequency suggested that reducing the symmetry through the non-isomorphic subgroup *P*23 removed the instability, while keeping the same cubic lattice symmetry. Figure 2 displays the eigenvector responsible for the rotation around the Zr-B bond for each of the BH_4^- units in the unit cell. Results have been verified by choosing different computational parameters. Both LDA and B3LYP functional were considered and various basis set and dispersion forces were taken into account, as reported in the Electronic Supplementary Information. In all cases, little changes in the value of the imaginary frequency have been obtained. Table 4 lists the geometrical parameters computed for the *P*23 space group, which are also rather close to the experimental values reported in Tables 2 and 3. The only relevant change is a slight expansion of the unit cell volume when passing from *P*-43*m* to *P*23 symmetry and rotation of each BH_4^- group by 17° around the B-Zr bond. From the energetic point of view, the difference in the

electronic energy between the two structures is about 20 kJ mol^{-1} per formula unit, in favor of the *P*23 polymorph, meaning that only 5 kJ mol^{-1} are associated to the rotation of each BH_4^- group.

Table 4 Computed structural parameters, bond lengths, bond angles and the imaginary frequency (ν) - if present - for $Zr(BH_4)_4$ in the two cubic space groups, *P*-43m and *P*23. Data obtained with PBE functional and triple-zeta basis set.

$Zr(BH_4)_4$		
Space Group	*P*-43*m*	*P*23
a / Å	5.873	5.894
V / $Å^3$	202.6	204.8
D_c /g·cm^{-3}	1.230	1.217
ν/cm^{-1}	–254	/
M-B /Å	2.2979	2.2938
M-H2 /Å	3.4920	3.4878
M-H1 /Å	2.1431	2.1372
B-B /Å	3.7525	3.7457
B-H2 /Å	1.1941	1.1941
B-H1 /Å	1.2492	1.2501
H2-H2 /Å	2.603	2.640
H1-H1 /Å	1.991	1.991
H1-H2 /Å	2.038	2.040
M-B-H1 /°	66.948	66.830
M-H1-B /°	80.617	80.641
B-M-H1 /°	32.435	32.530
H1-B-H1 /°	105.665	105.532
H1-B-H2 /°	113.052	113.170

In order to verify the robustness of computed results, the same approach adopted for the $Zr(BH_4)_4$ has been applied to the isostructural compound $Hf(BH_4)_4$. Results showed the same phonon instability in Gamma point for the *P*-43*m* group, which was removed by lowering the symmetry to the *P*23. Similar results have been reported in a previous computational work, where the *P*-43*m* structure for $Hf(BH_4)_4$ was found to be unstable.[30] Computed structural data for both space groups are reported in the Electronic Supplementary Information.

There is an obvious discrepancy between the ab-initio results and the crystallographic experiment on the symmetry of the crystal structure. The experimental single crystal data unambiguously find

the high-symmetry space group *P*-43*m*, while maintaining this symmetry in the theoretical calculations gives rise to an imaginary frequency. The difference between the two structures is in the slight rotation of each BH_4^- units around the B-Zr bond. Because of equivalence between the clockwise and anti-clockwise rotation one ends up with a structure containing half of the molecules in one state and the other half in the other (static disorder) or a structure in which the two conformations oscillate rapidly between the two minimum energy units (dynamic disorder); these two types of disorder cannot be distinguished by X-ray diffraction carried out at only one temperature. Indeed, the energy needed to rotate each BH_4^- is calculated to be small (5 kJ mol^{-1}, *vide supra*) enough for the rotation to occur almost freely even at the temperature of the X-ray experiment (100 K), in agreement with NMR data.[31] The X-ray experiment time scale is long compared to the time scale for the structural dynamics. Therefore, only the average structure with the electron density from each H atom distributed over the two H position in a symmetric way is observed (the distance between the two theoretically calculated H position is 0.66 Å). This causes the higher symmetry *P*-43*m* of the experimentally determined structure. However, refinement of a model using anisotropic thermal parameters for H1 leads to slightly lower residuals and clearly shows the largest movement perpendicular to the Zr-H line with an amplitude displacement of 0.3 Å. The observed thermal vibrations and atomic displacement ellipsoids may indicate orientational disorder (hindered rotations) of the BH_4^- groups. Large libration amplitudes is also observed for the hexagonal phase of lithiumborohydride, both by diffraction and nuclear magnetic resonance spectroscopy.ref1 An entropy contribution from disorder may contribute as a structural stabilizing factor, which is suggested to be the case for the hexagonal structure of $LiBH_4$.Ref2

Thus, experimental and theoretical data are in accord and clearly support that solid $Zr(BH_4)_4$ indeed consists of discrete neutral molecules of $Zr(BH_4)_4$. The molecules are expected to interact by weak van der Waals or dispersion interactions. However, the shortest distance between neighboring $Zr(BH_4)_4$ molecules in the solid is defined by the relatively short H2…H2 distances of 2.77 and 2.60 Å (experimental and theoretical values, respectively). These values are comparable to the B–H···H–B bond distances 2.33, 2.63 and 2.73 Å observed for the molecular borohydrides $Al(BH_4)_3$ [32,33], $Hf(BH_4)_4$ [26] and $Be(BH_4)_2$ [34], respectively. The hydrogen atoms participating in these interactions have the same partial charge in contrast to those in $LiBH_4{\cdot}NH_3$, with $B–H^{\delta-}\cdots{}^{+\delta}H–N$ bond distances of approximately 2.3 and 2.5 Å.[35] These latter dihydrogen bonds are significantly weaker as compared to the three $O–H^{\delta+}\cdots{}^{-\delta}H–B$ dihydrogen bonds in $NaBH_4{\cdot}2H_2O$,[36] with distances in the range 1.77 to 1.95 Å. The large thermal vibrations observed experimentally and the disorder suggested theoretically may reflect possible dynamic disorder, which minimize repulsive B–H···H–B interactions and maximize the structural entropy, which may be of significant importance for the properties of solid $Zr(BH_4)_4$.

4.3 *In situ synchrotron radiation powder X-ray diffraction*

$LiBH_4$-$ZrCl_4$ (6:1, S2) was studied in the temperature range from 19 to 60 °C using *in situ* SR-PXD, see Figure 3. All $ZrCl_4$ has reacted during ball milling to form $Zr(BH_4)_4$ and LiCl and the first diffractogram shows diffraction from $Zr(BH_4)_4$, LiCl and excess $LiBH_4$. The diffraction from $Zr(BH_4)_4$ disappears at T = 29 °C, in agreement with the reported melting point of 28.7 °C.[9] No crystalline or amorphous decomposition products seem to form since no change in the background of the SR-PXD data is observed. This may indicate a sublimation of $Zr(BH_4)_4$ rather than formation of a melt, which is also observed in previous studies.[12] Bragg reflections from $LiBH_4$ and LiCl

remain with nearly constant intensity to the end of the experiment at 60 °C. The Rietveld refinement profile of the first diffractogram measured at T = 19 °C is shown in Figure 4 and reveals a sample composition of $Zr(BH_4)_4$ (15 wt%), $LiBH_4$ (29 wt%) and LiCl (56 wt%), which indicates that some of the formed $Zr(BH_4)_4$ has evaporated from the sample.

4.3 *Infrared spectroscopy*

Infrared spectra were recorded at *RT* of $LiBH_4$–$ZrCl_4$ (4:1, S1) directly after the synthesis and after a time period of 5 to 120 min at *RT*, see Figure 5. For comparison, an IR spectrum was also measured for pristine $LiBH_4$, see Figure S2 in the supplementary information. The first spectrum, 0 min after the synthesis, shows three strong asymmetric B–H stretching modes at 2563, 2177 and 2112 cm^{-1} assigned to $Zr(BH_4)_4$. A weak IR-absorption band is found at ~2307 cm^{-1} assigned to the asymmetric BH stretching mode for excess $LiBH_4$ in the sample. The H–B–H bending of $Zr(BH_4)_4$ is found at 1207 cm^{-1}, where $LiBH_4$ has several modes with the strongest at ~1281 and ~1058 cm^{-1}. At the low frequency region an H–B–H bending mode of $Zr(BH_4)_4$ is observed at 494 cm^{-1} and LiCl stretch below 450 cm^{-1}. The spectra collected 5 to 120 min after the synthesis shows a significant decrease in the intensity of the H–B–H bending at 1207 and 494 cm^{-1} and also the asymmetric B–H stretching modes at 2563, 2177 and 2112 cm^{-1} suggesting that $Zr(BH_4)_4$ is evaporating at *RT* from the solid sample, see Figure 5.

In a recent paper, the predicting power of quantum-mechanical methods for computing and assigning the band features of rather complex borohydrides was demonstrated.[37] The simulated IR spectra of $Zr(BH_4)_4$ are shown in Figure 6 for *P*-43*m* and *P*23 space group symmetries. For BH_3, it has been demonstrated by a complete quantum mechanical treatment that harmonic frequencies are

in error by about 100 cm^{-1} with respect to the fundamental ones.[38] By assuming similar anharmonicity between the BH_3 modes and those of the BH_4^- moiety in the $Zr(BH_4)_4$ crystal a single scaling factor has been applied to all harmonic frequencies, calculated as the ratio between experimental [39] and PBE B–H asymmetric stretching labelled ν3 (see reference [38]) for the BH_3 molecule. The spectra calculated for *P*-43*m* and *P*23 structures are rather similar. As expected, lowering the symmetry from *P*-43*m* to *P*23 causes the splitting of a number of bands. For instance, while for the *P*-43*m* symmetry the most intense band, corresponding to the H–B–H bending, is at 1071 cm^{-1}, in the *P*23 the most intense (still H–B–H bending) is at 1098 cm^{-1}. On the other hand, the highest frequency values coincide in both cases at 2598 cm^{-1} (B–H stretching), while the other modes between 2958 and 1200 cm^{-1} are upshifted for the *P*23 structure by about 15 cm^{-1} as an average. It is worth noting that the calculated Born charges turn out equal to –0.2247 *e* and –0.0535 *e* for H1 and H2 atom, respectively, suggesting an almost neutral character for H2. In the lowest frequency region of the IR spectra, the most intense band is at 455 cm^{-1} for *P*-43*m* and at 487 cm^{-1} for the *P*23.

Assuming the *P*23 structure as the reference, a comparison with experiment is only possible with the spectrum of the $LiBH_4$–$ZrCl_4$ (4:1) powder (sample S1) and the reported $Zr(BH_4)_4$ molecule recorded in gas-phase,[12] as the infrared spectrum of the corresponding crystal is missing. The comparison reveals that: i) the high frequency B–H asymmetric stretching mode of 2598 cm^{-1} is close to the experimental values of 2563 and 2575 cm^{-1} for solid and gas-phase $Zr(BH_4)_4$, respectively; ii) the two asymmetric B–H stretching modes at 2239 and 2195 cm^{-1} are higher with respect to the experimental values of 2177 and 2112 cm^{-1} for solid-phase and 2194 and 2133 cm^{-1} for gas-phase $Zr(BH_4)_4$; iii) the most intense H–B–H bending mode at 1098 cm^{-1} is definitely lower than the experimental values of 1207 and 1218 cm^{-1} for solid and gas-phase $Zr(BH_4)_4$, respectively.

These results show that, besides the intrinsic deficiencies of the PBE functional and rather crude treatment of the anharmonicity, the crystal field present in the calculated spectrum is mainly responsible of the deviations between the two datasets. The simulated IR spectrum of $Hf(BH_4)_4$ are also reported in the Electronic Supplementary Information.

5. Conclusion

Zirconium borohydride, $Zr(BH_4)_4$, a volatile molecular material, is studied by single crystal X-ray diffraction and theoretical structural optimization using DFT. The structure consists of discrete $Zr(BH_4)_4$ molecules separated by H···H distances of 2.77 and 2.60 Å for experimental and calculated values, respectively. *Ab initio* calculations indicate disorder dynamics in the structure of $Zr(BH_4)_4$, possibly due to motion of BH_4^- complex anions. Large thermal vibrations observed experimentally and the disorder suggested theoretically may reflect possible dynamic disorder, which minimize repulsive B–H···H–B interactions and maximize the structural entropy, which may be of significant importance for the properties of solid $Zr(BH_4)_4$. [B1]Calculated geometrical parameters and IR data for the two suggested structural symmetries are very similar. *In situ* synchrotron radiation powder X-ray diffraction suggest that solid $Zr(BH_4)_4$ decompose by sublimation.

Acknowledgements

The authors would like to acknowledge funding for this research from the European Community's Seventh Framework Program FP7/2007-2013 under grant agreement No 226943-FLYHY. The Danish Research Council for Natural Sciences (Danscatt) is also thanked for financial support. The work was supported by the Danish National Research Foundation (Centre for Materials

Crystallography), the Danish Strategic Research Council (Centre for Energy Materials) and the Carlsberg Foundation. The access to beam time at the MAX-II synchrotron, Lund, Sweden in the research laboratory MAX-lab is gratefully acknowledged. We thank Prof. Davide Viterbo (Università Piemonte Orientale, Alessandria, Italy) for fruitful discussion.

Supporting Information Available: The experimental IR spectrum of $LiBH_4$-$ZrCl_4$ compared with $LiBH_4$ and Computational details, *e.g.* the computed structural data for the $Zr(BH_4)_4$ and $Hf(BH_4)_4$ in space groups *P*23 and *P*-43*m*, and the simulated IR spectrum of $Hf(BH_4)_4$. This information is available free of charge via the Internet at http://pubs.acs.org.

References

(1) Orimo, S. I.; Nakamori, Y.; Eliseo, J. R.; Züttel, A.; Jensen, C. M. *Chem. Rev.* **2007**, *107*, 4111–4132.
(2) Ravnsbæk, D. B.; Filinchuk, Y.; Černý, R.; Jensen, T. R. *Z. Kristallogr.* **2010**, *225*, 557–569.
(3) Rude, L. H.; Nielsen, T. K.; Ravnsbæk, D. B.; Bösenberg, U.; Ley, M. B.; Richter, B.; Arnbjerg, L. M.; Dornheim, M.; Filinchuk, Y.; Besenbacher, F.; Jensen, T. R. *Phys. Status Solidi* **2011**, *208*, 1754–1773.
(4) Ravnsbæk, D. B.; Filinchuk, Y.; Cerenius, Y.; Jakobsen, H. J.; Besenbacher, F.; Skibsted, J.; Jensen, T. R. *Angew. Chem. Int. Ed.* **2009**, *48*, 6659–6663.
(5) Filinchuk, Y.; Richter, B.; Jensen, T. R.; Dmitriev, V.; Chernyshov, D.; Hagemann, H. *Angewandte Chemie* **2011**, *123*, 11358–11362.
(6) Černý, R.; Penin, N.; Hagemann, H.; Filinchuk, Y. *J. Phys. Chem. C* **2009**, *113*, 9003–9007.
(7) Ravnsbæk, D. B.; Filinchuk, Y.; Černý, R.; Ley, M. B.; Haase, D.; Jakobsen, H. J.; Skibsted, J.; Jensen, T. R. *Inorg. Chem.* **2010**, *49*, 3801–3809.
(8) Rude, L. H.; Filinchuk, Y.; Sørby, M. H.; Hauback, B. C.; Besenbacher, F.; Jensen, T. R. *J. Phys. Chem. C* **2011**, *115*, 7768–7777.
(9) Hoekstra, H. R.; Katz, J. J. *J. Am. Chem. Soc* **1949**, *71*, 2488–2492.
(10) Nakamori, Y.; Li, H.; Miwa, K.; Towata, S. I.; Orimo, S. I. *Mater. Trans.* **2006**, *47*, 1898–1901.
(11) Nöth, H. *Angewandte Chemie* **1961**, *73*, 371–383.
(12) Gennari, F. C.; Fernández Albanesi, L.; Rios, I. J. *Inorg. Chim. Acta* **2009**, *362*, 3731–3737.
(13) Suryanarayana, C. *Progr. Materials Sci.* **2001**, *46*, 1–184.
(14) Balema, V. P. *Mater. Matt.* **2007**, *2*, 16–18.
(15) Sheldrick, G. M. *Acta Cryst. A* **2008**, *64*, 112–122.
(16) Cerenius, Y.; Stahl, K.; Svensson, L. A.; Ursby, T.; Oskarsson, A.; Albertsson, J.; Liljas, A. *J. Synchrotron Radiat.* **2000**, *7*, 203–208.
(17) Jensen, T. R.; Nielsen, T. K.; Filinchuk, Y.; Jørgensen, J. E.; Cerenius, Y.; Gray, E. M.; Webb, C. J. *J. Appl. Cryst.* **2010**, *43*, 1456–1463.
(18) Hammersley, A. P.; Svensson, S. O.; Hanfland, M.; Fitch, A. N.; Hausermann, D. *High Pressure Res.* **1996**, *14*, 235–248.
(19) Rodriguez-Carvajal, J. *FULLPROF SUITE: LLB Sacley & LCSIM Rennes*; France, 2003.

(20) Dovesi, R.; Roetti, V. R.; Orlando, R.; Zicovich-Wilson, C. M.; Pascale, F.; Civalleri, B.; Doll, K.; Harrison, N. M.; Bush, I. J.; D'Arco, P.; Llunell, M. *CRYSTAL2009 User's Manual (http://www.crystal.unito.it)*; University of Torino, Torino, 2009.
(21) Perdew, J. P.; Burke, K.; Ernzerhof, M. *Phys. Rev. Lett.* **1996**, *77*, 3865–3868.
(22) Dovesi, R. *Zirconium Basis-sets, unpublished, web: http://www.crystal.unito.it/Basis_Sets/zirconium.html*.
(23) Schäfer, A.; Huber, C.; Ahlrichs, R. *J. Chem. Phys.* **1994**, *100*, 5829.
(24) Pascale, F.; Zicovich-Wilson, C. M.; López Gejo, F.; Civalleri, B.; Orlando, R.; Dovesi, R. *J. Comput. Chem.* **2004**, *25*, 888–897.
(25) Zicovich-Wilson, C. M.; Torres, F. J.; Pascale, F.; Valenzano, L.; Orlando, R.; Dovesi, R. *J. Comput. Chem.* **2008**, *29*, 2268–2278.
(26) Broach, R. W.; Chuang, I. S.; Marks, T. J.; Williams, J. M. *Inorg. Chem.* **1983**, *22*, 1081–1084.
(27) Bird, P. H.; Churchill, M. R. *Chem. Commun. (London)* **1967**, *8*, 403.
(28) Filinchuk, Y.; Chernyshov, D.; Černý, R. *J. Phys. Chem. C* **2008**, *112*, 10579–10584.
(29) Soulie, J. P.; Renaudin, G.; Černý, R.; Yvon, K. *J. Alloys Compd.* **2002**, *346*, 200–205.
(30) Nakamori, Y.; Miwa, K.; Ninomiya, A.; Li, H.; Ohba, N.; Towata, S.; Züttel, A.; Orimo, S. I. *Phys. Rev. B* **2006**, *74*, 45126.
(31) Blanchard, D.; Marosson, J. B.; Riktor, M. D.; Kheres, J.; Sveinbjörnsson, D.; Bardaji, E. G.; Leon, A. N.; Juranyi, F.; Wuttke, J.; Lefmann, K.; others *J. Phys. Chem. C* **2012**, *116*, 2013–2023.
(32) Miwa, K.; Ohba, N.; Towata, S.; Nakamori, Y.; Züttel, A.; Orimo, S. I. *J. Alloys Compd.* **2007**, *446-447*, 310–314.
(33) Aldridge, S.; Blake, A. J.; Downs, A. J.; Gould, R. O.; Parsons, S.; Pulham, C. R. *J. Chem. Soc., Dalton Trans* **1997**, 1007–1012.
(34) Marynick, D. S.; Lipscomb, W. N. *Inorg. Chem.* **1972**, *11*, 820–823.
(35) Johnson, S. R.; David, W. I. F.; Royse, D. M.; Sommariva, M.; Tang, C. Y.; Fabbiani, F. P. A.; Jones, M. O.; Edwards, P. P. *Chem.-Asian J.* **2009**, *4*, 849–854.
(36) Filinchuk, Y.; Hagemann, H. *Eur. J. Inorg. Chem.* **2008**, *20*, 3127–3133.
(37) Zavorotynska, O.; Corno, M.; Damin, A.; Spoto, G.; Ugliengo, P.; Baricco, M. *J. Phys. Chem. C* **2011**, *115*, 18890–18900.
(38) Schuurman, M. S.; Allen, W. D.; Schaefer III, H. F. *J. Comput. Chem.* **2005**, *26*, 1106–1112.
(39) Kawaguchi, K. *J. Chem. Phys.* **1992**, *96*, 3411.

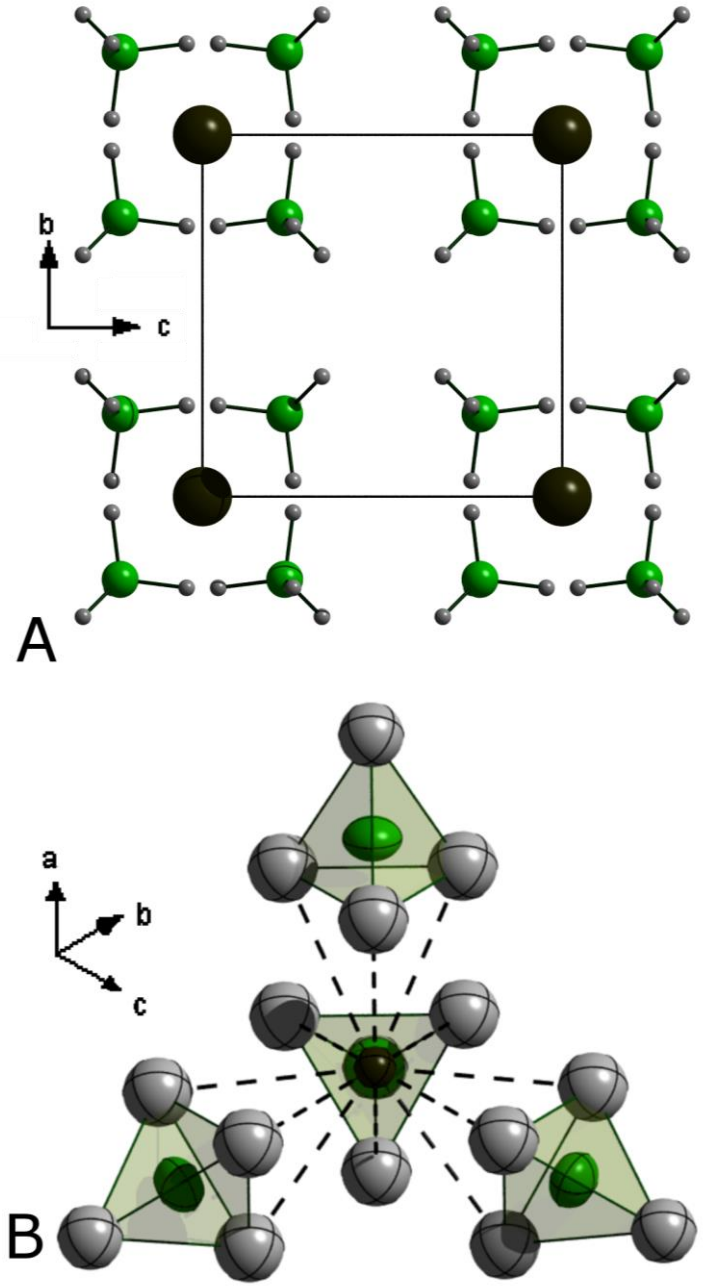

Figure 1. A) Illustration of the cubic crystal structure of $Zr(BH_4)_4$. **B**) the tetrahedral coordination of Zr by face-sharing with four BH_4 tetrahedra. The ellipsoids are shown at 50 % probability level. Zirconium is shown as black spheres, boron as green and hydrogen as grey spheres.

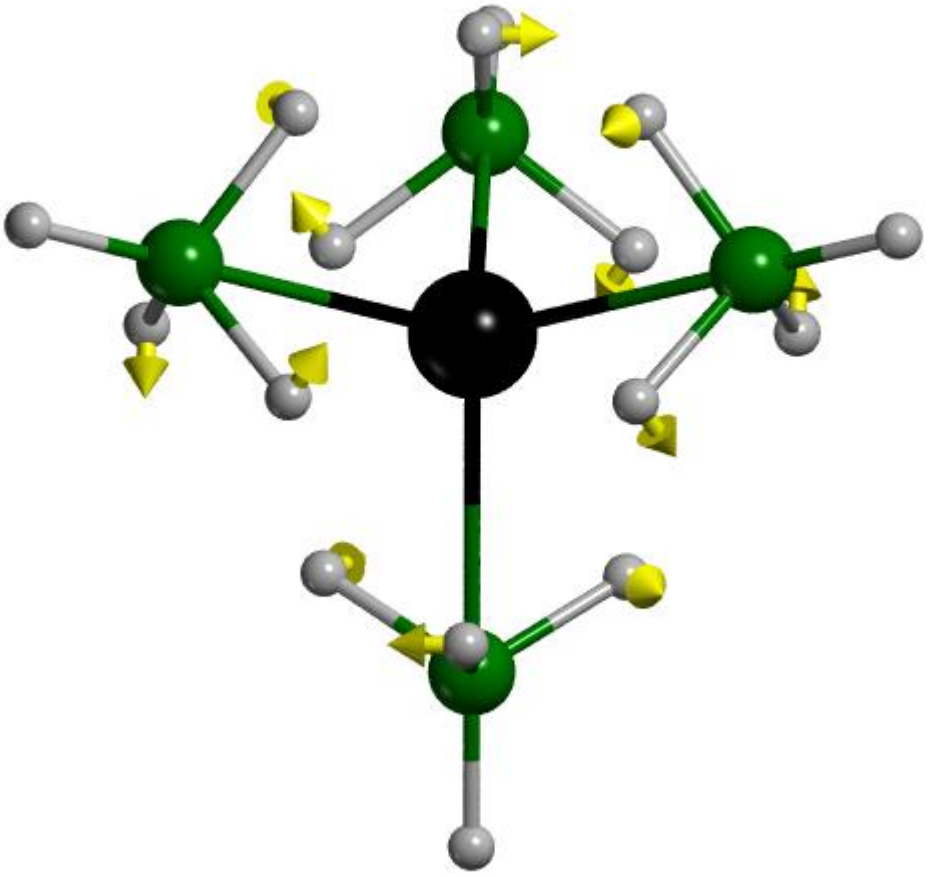

Figure 2. Graphical visualization of the eigenvector associated to the computed imaginary frequency for $Zr(BH_4)_4$ within the *P*-43*m* space group. Zirconium is shown as a black sphere, boron as green and hydrogen as grey spheres. Yellow arrows indicate the direction of the hindered rotational motion.

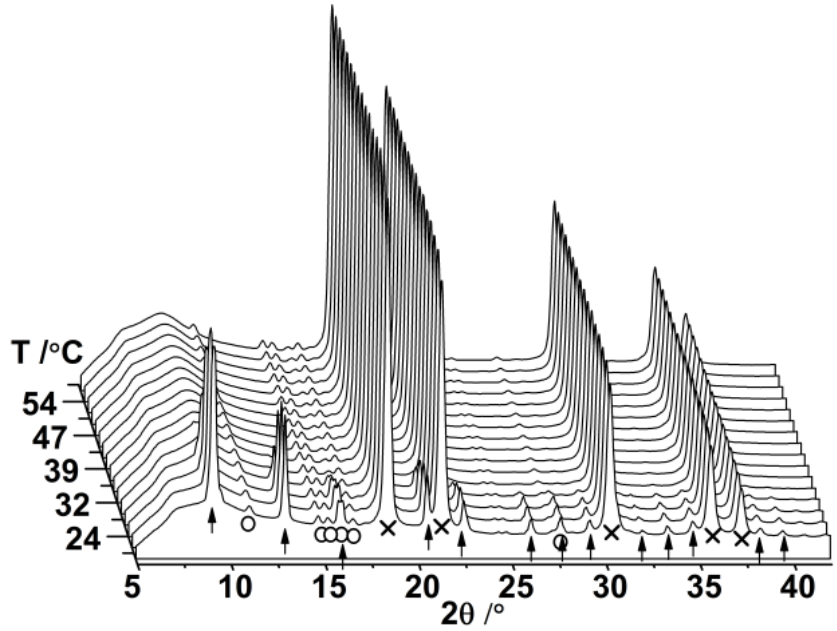

Figure 3. *In situ* synchrotron radiation powder X-ray diffraction (SR-PXD) data measured for $LiBH_4$–$ZrCl_4$ (6:1, S2) heated from 19 to 60 °C (heating rate 2.5 °C/min, λ = 0.94499 Å). Symbols: ○ *o*-$LiBH_4$, × LiCl and ▲ $Zr(BH_4)_4$.

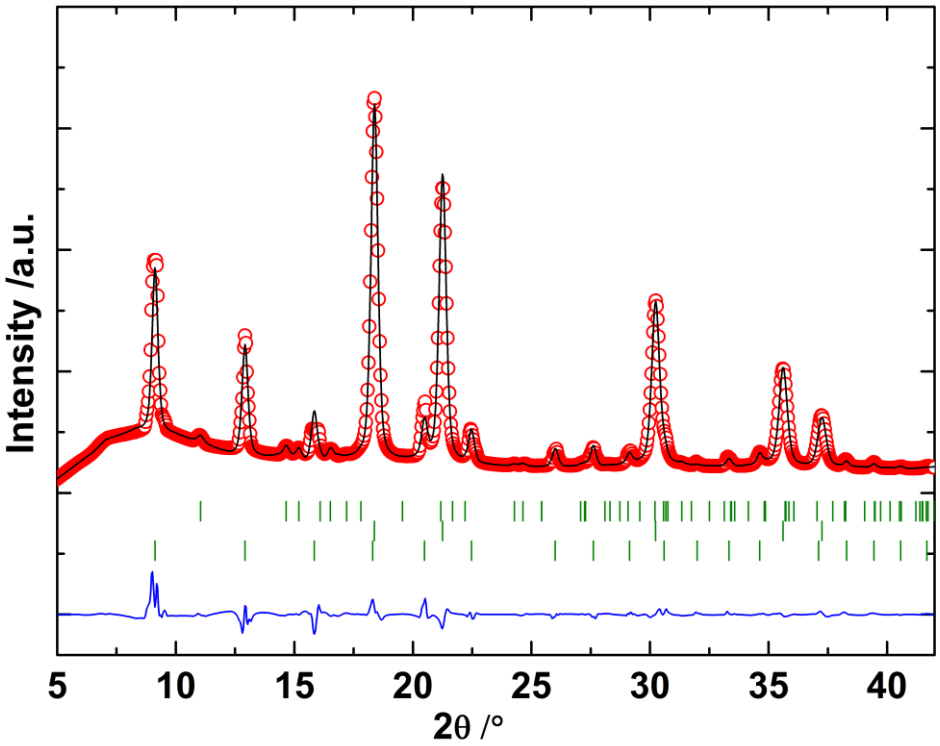

Figure 4. Rietveld refinement profile of $LiBH_4$–$ZrCl_4$ (6:1, S2) measured at 19 °C by SR-PXD, see Figure 3 (λ = 0.94499 Å). Tic marks: *o*-$LiBH_4$ (top), LiCl (middle) and $Zr(BH_4)_4$ (bottom).

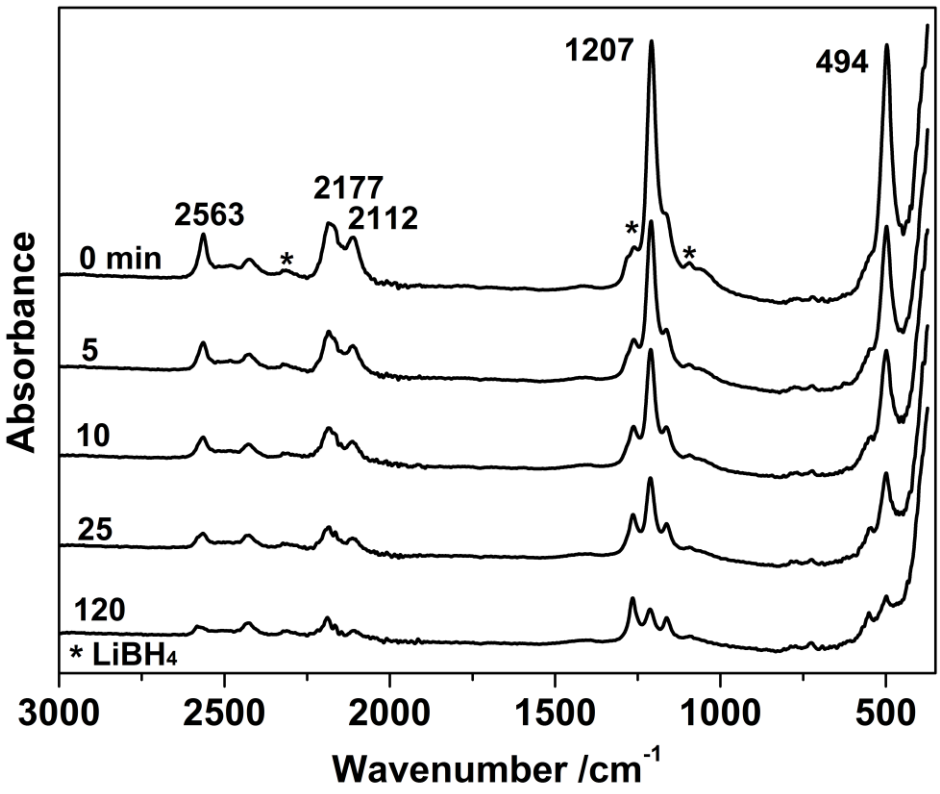

Figure 5. FT-IR spectra of $LiBH_4$-$ZrCl_4$ (4:1, S1) measured at *RT* and 0, 5, 10, 25 and 120 min after the synthesis. The baseline of the spectra has been displaced for clarity.

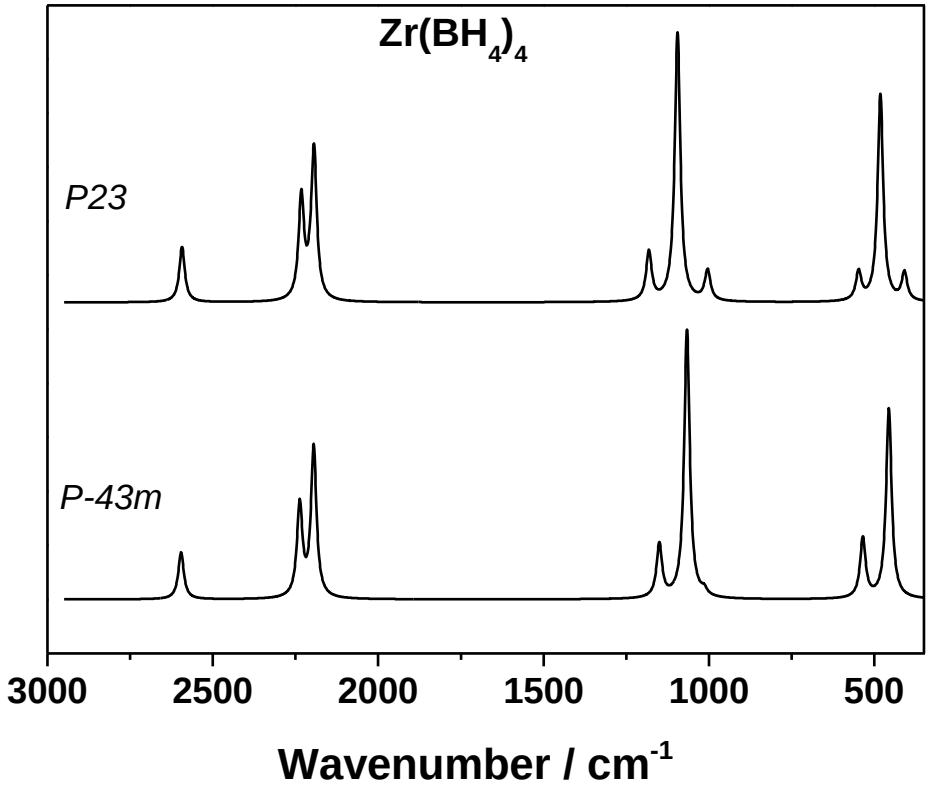

Figure 6. Computed IR spectra for $Zr(BH_4)_4$ structures: bottom, *P*-43*m* symmetry; top: *P*23 symmetry.